Available online at www.sciencedirect.com
SCIENCE DIRECT®
Journal of Nuclear Materials 327 (2004) 202–210
journal of nuclear materials
www.elsevier.com/locate/jnucmat

Damage and dynamic strain aging in a thermal aged cast duplex stainless steel

V. Calonne [a], C. Berdin [b,*], B. Saint-Germain [b], S. Jayet-Gendrot [a]

[a] E.D.F., Division Recherche et Développement, Site des Renardières, F-77818 Moret sur Loing cedex, France
[b] Laboratoire MSS/Mat CNRS 8579, Ecole Centrale Paris, Grande Voie des Vignes, F-92295 Châtenay Malabry cedex, France

Received 22 September 2003; accepted 12 February 2004

Abstract

An experimental study was carried out at 320 °C in order to determine the damage kinetics of a thermal aged duplex stainless steel. Compression and tensile tests were performed at 320 °C and at 20 °C for comparison. Typical steps of damage for this material were found at room temperature. At 320 °C, no bulk damage was observed, but strain and damage were localized. The experimental mechanical results revealed the existence of dynamic strain aging. The absence of bulk damage is linked to this phenomenon: as soon as damage appears in ferrite, there is localization and fracture follows.

1. Introduction

Type CF8M duplex stainless steels are used for the fabrication of cast components for the reactor cooling system of pressurized water reactor. The ferrite phase of these materials is known to be susceptible to thermal aging at about 320 °C which is the operating temperature [1–6]. Austenite, the major phase, remains ductile but ferrite hardens and embrittles, inducing a significant decrease in toughness and tensile ductility [6]. Moreover, casting defects which can act as crack initiation sites, have been evidenced in large cast components [7,8].

In support to safety analyses, the possibility of long crack propagation by ductile tearing was studied [9,10]. The testing standard [11] requires large specimens that makes tests expensive and difficult to run. So, an effort was made to predict crack propagation using local approach as for example the Gurson's model modified by Tvergaard and Needleman [12–14]. In this model, the effect of the damage evolution on the stress distribution is taken into account. The behavior and the damage mechanisms of duplex stainless steels have therefore to be studied. Such a study was already performed at room temperature: the damage of the bulk material stems from voids initiated by cleavage within the ferrite phase [15]. Joly et al. [15] followed by Besson et al. [16] proposed the void volume fraction driven by the plastic strain as the physical damage variable. However, the operating temperature of the cast duplex stainless steel components is about 320 °C. Previous studies performed at this temperature showed that the fracture does not exactly come from the same mechanisms as those observed at room temperature [17,18]. So, further insights into the damage mechanisms at the operating temperature are needed in order to suggest a damage mechanical model predicting the crack propagation strength.

This paper deals with the study of aged duplex stainless steels behavior, damage and fracture at 320 °C. Results obtained at 20 °C is reminded here for comparison purpose. The paper is divided into three sections: the first one presents the experimental details, the second shows the results of mechanical testings as well as damage observations, and the third section is devoted to the discussion.

* Corresponding author. Tel.: +33-01 4113 1325; fax: +33-01 4113 1430.
E-mail address: berdin@mssmat.ecp.fr (C. Berdin).

0022-3115/$ - see front matter © 2004 Elsevier B.V. All rights reserved.
doi:10.1016/j.jnucmat.2004.02.010

Nomenclature

F	applied load	ε	total strain
S	specimen section	$\dot{\varepsilon}$	strain rate
h	specimen height	σ	stress
h_0	initial specimen height	R_p	yield strength
α	ferrite	R_m	ultimate strength
γ	austenite	A	fracture strain

2. Experimental details

2.1. Material

The studied duplex stainless steel was statically cast in the shape of large plates and aged for 2 500 h at 400 °C. Its chemical composition (wt%) is 0.029 C, 0.046 N, 21.65 Cr, 10.05 Ni, 2.66 Mo, 1.33 Si, 0.83 Mn, 0.025 P, 0.004 S. The ferrite volume fraction is around 32%. Charpy impact energy is 1.4 and 3.5 daJ/cm^2 at 20 and 320 °C respectively. These values associated to microhardness measurements on the ferrite phase (about 400 $H_{v\ 100\ g}$ showed that the material is severely embrittled.

Because of the static casting manufacturing process, the solidification structure is columnar close to the mould surface and equiaxed in the bulk (Fig. 1). Columnar grains are oriented along $\langle 1\,0\,0\rangle\alpha$ crystallographic directions. Equiaxed ones reveal no preferential orientation [19]. Their size is very large: generally around 2 or 3 mm in diameter. The microstructure studied by optical microscopy (Fig. 2) confirms the complex morphology of the ferrite (α) and austenite (γ) [19]: the two phases are bipercolated and linked by crystallographic orientation relationships which are close to those given by Kurdjumov and Sachs [20], typically $[1\,1\,0](1\,\bar{1}\,1)\gamma\|[1\,1\,1](1\,\bar{1}\,0)\alpha$.

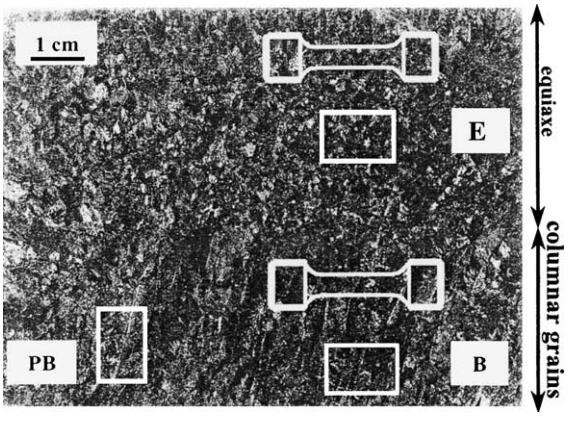

Fig. 1. Solidification structure of statically cast duplex stainless steel and specimens sampling.

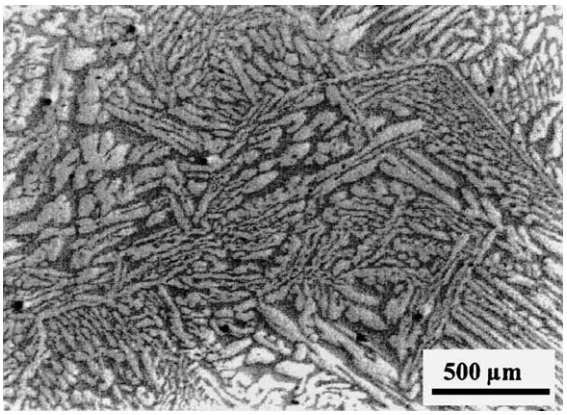

Fig. 2. Microstructure of equiaxed grains in statically cast duplex stainless steel. The ferrite appears in dark grey and the austenite, in light grey.

2.2. Specimens and experiments

Tensile tests were performed on smooth cylindrical specimens 6 mm in diameter and 20 mm in gauge length. Cylindrical specimens (height 18 mm and diameter 12 mm) were loaded in compression in order to detect a difference in damage mode according to the loading direction. The tests were performed at 320 °C and at room temperature for comparison. The influence of the structure from solidification on the mechanical behavior and on the fracture mechanisms was investigated: specimens were cut in such a way that the loading direction during the test was perpendicular to columnar (B) grains (Fig. 1). Compression specimens were small enough to be also cut parallel to columnar grains (PB).

Strain rate for tensile and compression tests was about 3×10^{-4} s^{-1}. In compression, the displacement $u(t)$ was computed in order to keep the strain rate constant during the test: $u(t) = h_0(1-\exp(\dot{\varepsilon}t))$ where h_0 is the initial height, t the current loading time and $\dot{\varepsilon}$, the strain rate. The maximum height reduction was about 50%. Friction between the machine and the specimen surfaces was reduced by application of a lubricant (boron nitride). In tensile tests, the strain was measured by a gauge extensometer at room temperature and calculated

from the machine crosshead displacement before being corrected by the loading machine stiffness for the tests carried out at 320 °C. At this temperature, the thermal gradient along the specimen was checked and was less than 3 °C. Three specimens were tested for each loading condition.

After testing, tensile fracture surfaces were observed by scanning electron microscopy (SEM). Tension and compression specimens were also cut parallel to the loading direction in order to observe the damage by optical microscopy. The sections were polished and etched with a solution made of 10 g of potassium ferricyanide and of 10 g of NaOH/caustic in 80 ml of water and heated to 80 °C.

3. Results

3.1. Tensile tests

True stress ($\sigma = F/S$)–true strain ($\varepsilon = \ln(1 + \Delta l/l_0)$) curves established for equiaxed and columnar materials at 320 °C are presented in Fig. 3. Tables 1 and 2 summarize the conventional tensile properties at 20 and 320 °C respectively.

At room temperature, the tensile fracture strains were small and no striction was observed. This is correlated with the high material embrittlement previously mentioned. They showed a wide scatter (2.8–6.6%) due to the coarse solidification structure. The number of loaded grains being smaller in columnar specimens (2 or 3 grains) than in equiaxed ones (5 or 6 grains), the scattering is larger for the columnar specimens.

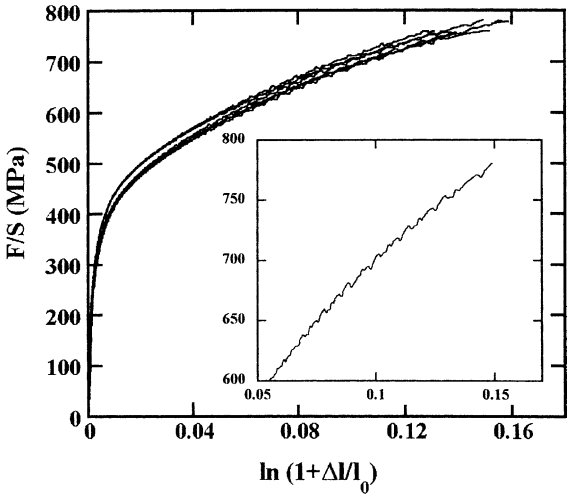

Fig. 3. True stress–true strain curves established at 320 °C for equiaxed and columnar grain specimens.

Table 1
Conventional tensile properties for equiaxed (E) and columnar grain (B) materials tested at 20 °C

	$R_{p0,2}$ (MPa)	R_m (MPa)	A (%)
E2	390	710	5.7
E3	380	655	2.8
E4	390	660	3.5
B1	360	660	5.3
B2	350	690	6.6
B3	460	720	4.7

Table 2
Conventional tensile properties for equiaxed (E) and columnar grain (B) materials tested at 320 °C

	$R_{p0,2}$ (MPa)	R_m (MPa)	A (%)
E5	340	670	17.1
E6	330	674	16.0
E7	340	660	15.0
B4	330	656	16.1
B5	370	672	12.6
B6	350	663	14.6

At 320 °C, the elongation scatter is less (12.6–17%) and the mean value is superior to the 20 °C one. Columnar and equiaxed materials exhibit the same tensile behavior. Above a strain of 4.5%, stress serrations which are characteristic of dynamic strain aging were observed (Fig. 3).

The fracture surfaces of the specimens tested at 20 and 320 °C were observed by scanning electron microscopy (Figs. 4 and 5). In both cases, the austenite fracture was ductile. At room temperature, the ferrite fracture occurred mainly by cleavage but sometimes also by shearing. At 320 °C, the fracture surface was divided in three areas, each one corresponding to a major ferrite fracture mechanism: cleavage, shearing or ductile fracture. These areas were 2 or 3 mm in dimensions. Thus they could correspond to ferrite grains or to some variants of ferrite/austenite Kurdjumov–Sachs relationships [21].

The damage was studied using polished and etched sections of equiaxed tensile specimens (Fig. 6).

At room temperature, the fracture occurred in three steps [15,17,22]: ferrite cleavage initiation, cleavage crack extension and growth in austenite. Cracks were gathered in clusters corresponding to cleavage favorable crystallographic relationships between austenite and ferrite (Fig. 6(a)) [15,21]. Such clusters were found far away from the fracture surface. No striction was visible.

By contrast, at 320 °C, the section showed almost no damage (Fig. 6(b)). Scarce cleavage cracks were observed just under the fracture surface (Fig. 6(c)) but no cluster of crack was found. Some cavities were also

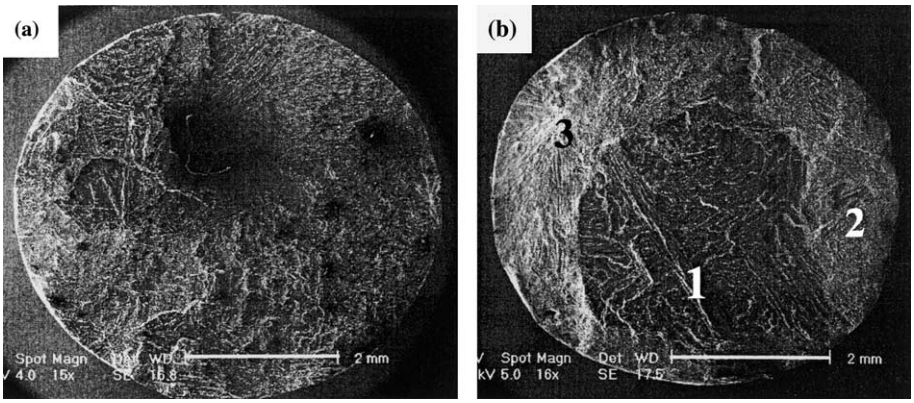

Fig. 4. Fracture surfaces of tensile specimens tested at 20 °C (a) and 320 °C (b). The latter surface is divided in three areas corresponding to the ferrite major fracture mechanisms: area 1 – cleavage, area 2 – shearing, area 3 – ductile fracture.

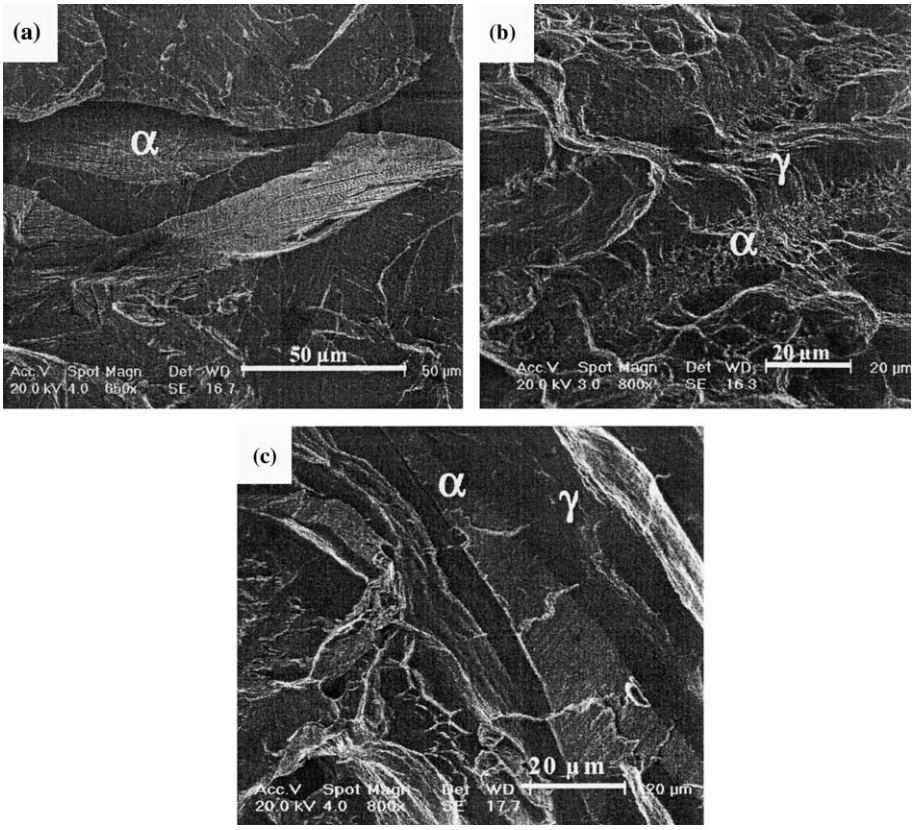

Fig. 5. Ferrite fracture observation at 320 °C: (a) cleavage, (b) ductile, (c) shearing fracture.

present. They could be initiated from precipitates or from micro-porosities. They were elongated in the tensile direction as can be seen in Fig. 6(b). Even at this temperature, no significant striction was seen.

3.2. Compression tests

True stress ($\sigma = F/S$)–true strain ($\varepsilon = \ln(1 + \Delta h/h_0)$) compression curves established for equiaxed and

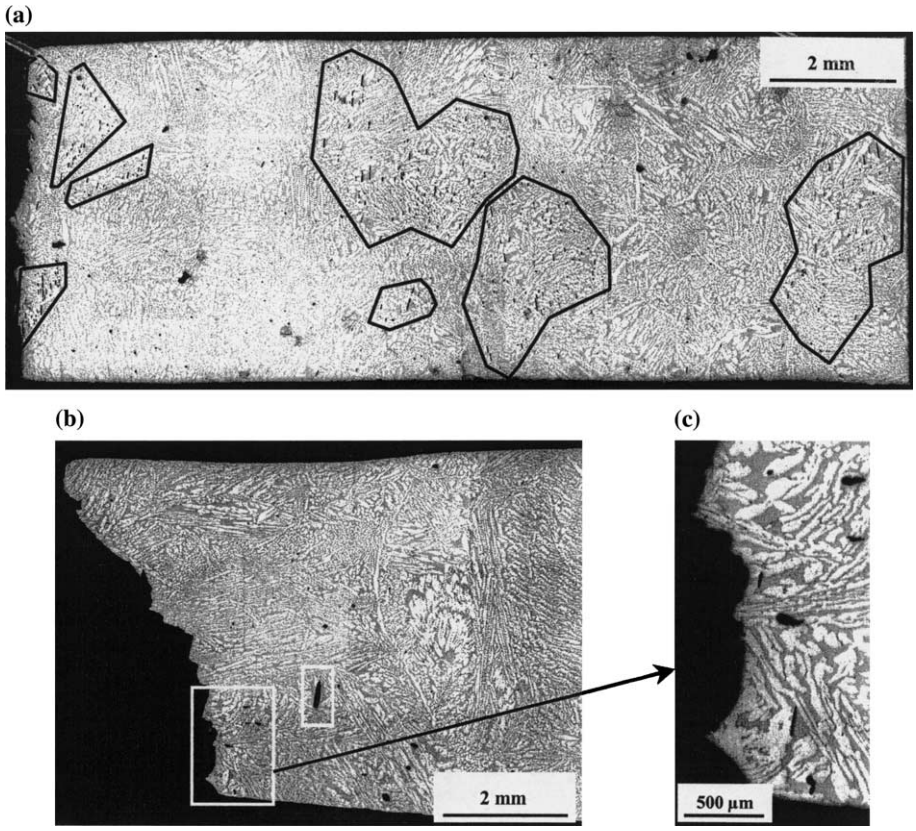

Fig. 6. Polished and etched longitudinal sections of equiaxed tensile specimens tested at (a) 20 °C (A% = 5.7%) and (b) 320 °C (A% = 16%). Details of the polished section of the specimen tested at 320 °C (c): non-opened cleavage cracks just below the fracture surface and cavities elongated in the loading direction. The ferrite appears in dark grey and the austenite, in light grey.

columnar specimens tested at 320 °C are presented in Fig. 7. No difference can be noticed between equiaxed and columnar materials. Moreover, on the common strain range, the stress levels reached in tension are close to those reached in compression. At room temperature, the maximum imposed strain was in the range of 50–60% and no instability was found. At 320 °C, the first tested specimen showed instabilities for strains higher than 25% and a macroscopic crack. The strain level was thus limited to 20% for the other tests.

Polished and etched sections of the specimens were observed. On a specimen tested at room temperature and for a strain level of 52% (Fig. 8), damage in the ferrite and also some intense shearing could be observed. Shearing was localized along the specimen diagonal. It consisted of a band 400 µm wide and it could be related to the macroscopic shearing of the specimen visible in Figs. 8 and 9. The damage consists of shearing cracks, cleavage cracks and also small cavities (Fig. 10). Shearing cracks developed mainly in ferrite and in the shearing band. Ferrite is less ductile than austenite and thus it easily fractures under intense strain. Cleavage cracks, commonly perpendicular to the main loading direction in tension, were in this case, parallel to the compression axis. Cavities could result from cleavage

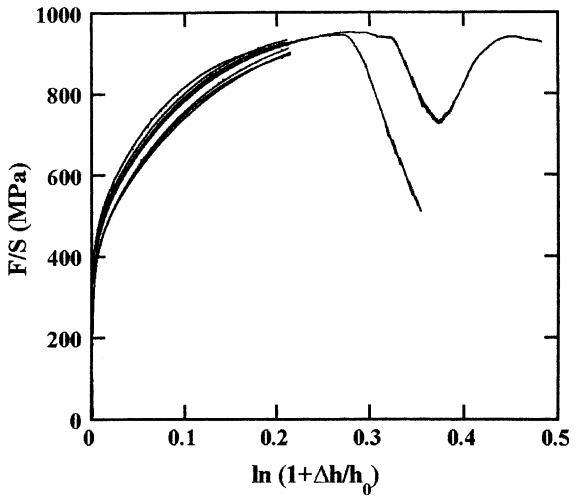

Fig. 7. True stress–true strain compression curves for equiaxed and columnar grain specimens tested at 320 °C.

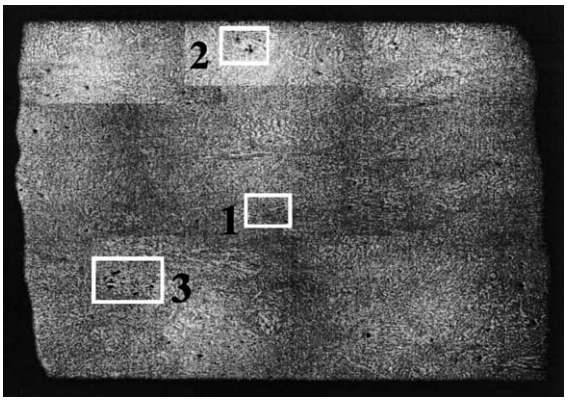

Fig. 8. Polished and etched longitudinal section of an equiaxed compression specimen tested at 20 °C. $\ln(1 + \Delta h/h_0) = 52\%$.

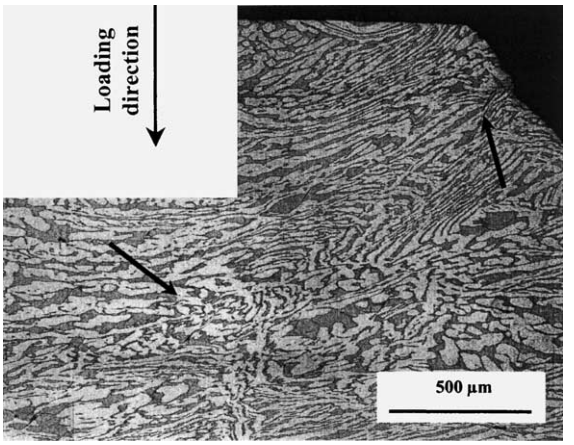

Fig. 9. Shear band along the diagonal of an equiaxed compression specimen tested at 20 °C. Detail of Fig. 8.

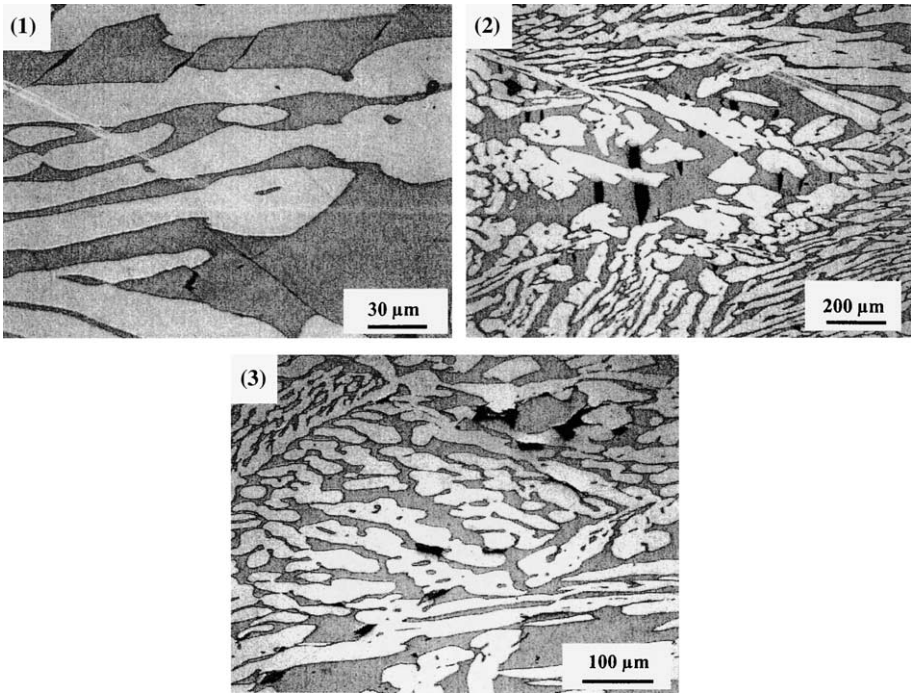

Fig. 10. Damage in an equiaxed compression specimen tested at 20 °C. Details 1, 2 and 3 of Fig. 8. (1) Shearing in ferrite, (2) cleavage in ferrite, (3) small cavities in ferrite.

cracks that were crushed and deformed. For lower strains (around 20%), the damage is assumed not to exist but this was not checked.

At 320 °C and for strains lower than 25%, the polished sections of the specimen are damage free (Fig. 11(a)). Nevertheless, for higher strains, a shear band appears along the specimen diagonal (Fig. 11(b)). The material flow, leads to the fracture of the specimen (Fig. 12). This fracture can explain the stress drop observed on the stress–strain curve. Except for the shear band, no damage in the specimen could be detected.

4. Discussion

Typical steps of damage were observed on polished sections of the tensile specimens tested at room temperature.

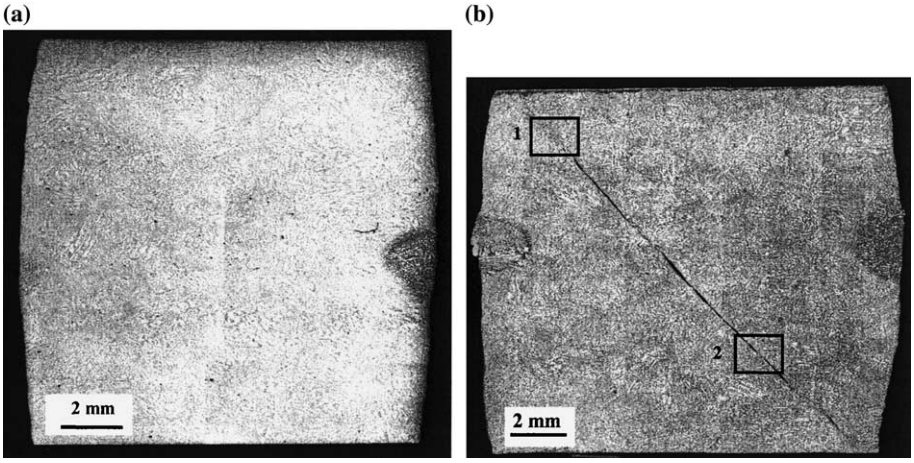

Fig. 11. Polished and etched longitudinal section of an equiaxed compression specimen tested at 320 °C. (a) $\ln(1 + \Delta h/h_0) = 22\%$, (b) $\ln(1 + \Delta h/h_0) = 36\%$.

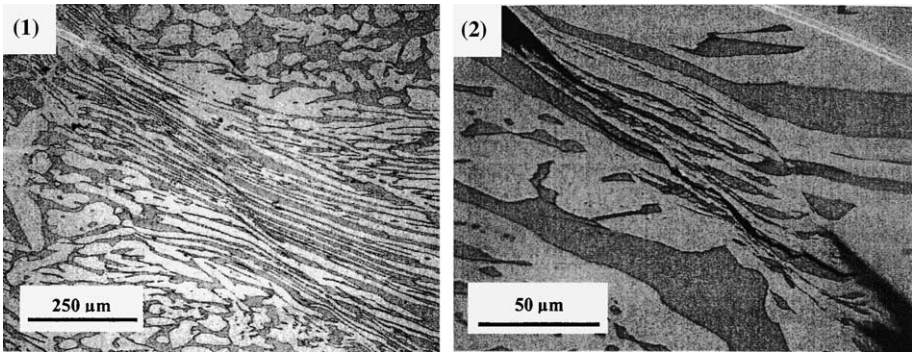

Fig. 12. Shearing along the diagonal of a columnar compression specimen tested at 320 °C. Details 1 and 2 of Fig. 11.

Nevertheless, after compression tests carried out up to a strain of 52%, some damage was observed for the first time ever (as far as the authors know) in these materials. This damage consists of cleavage cracks parallel to the loading direction and located in the center of the specimen. Cleavage cracks are commonly perpendicular to the positive maximum principal stress for metallic materials in tension. In compressive loading, a local positive stress usually occurs on the equatorial surface because of the barreling of the specimen [23]. However, as can be seen in Fig. 8, the specimen was not barreled, and cleavage cracks were not found on the equatorial surface. This kind of damage can be linked to the material features. First, local crystallographic orientations in this coarse solidification structure might modify the stress field and the ferrite can be locally in a state of tension in the radial direction of the specimen. Next, the radial direction being the flow direction of the material during the test, it confirms that, from a macroscopic viewpoint, the plastic strain drives the damage nucleation in this material [15].

At 320 °C no damage was observed far away from the fracture surface of the tensile specimen. The compression specimen presented a macroscopic crack and some intense shearing inside even though the global shape was not sheared. Mechanical testings revealed a jerky flow in the tensile test with stress serrations and a sudden large load drop in compression. All these observations can be explained by dynamic strain aging. Dynamic strain aging was already found by other authors when carrying out tensile tests on similar duplex stainless steels at 320 °C with strain rates in the range of 10^{-1}–10^{-4} s^{-1} [24]. The magnitude of this phenomenon depends on temperature, strain and strain rate. It is commonly observed in austenitic steels tested in the temperature range of 200–550 °C [25–27] and in ferritic steels tested from 150 to 300 °C [28]. This raises the question whether dynamic aging is linked to ferrite or to austenite.

Dynamic strain aging in steel is characterized by an increase in strain hardening, a decrease in fracture strain and fracture toughness [28], but also by a decrease in strain rate sensitivity which can become negative [29]. Negative strain rate sensitivity leads to localized deformation and instability. As a consequence, in tensile tests at 320 °C, as soon as cleavage cracks occur in ferrite, so does localization. Thus almost no striction is observed and no bulk damage appears. In fact, it is difficult to determine whether damage nucleation leads to strain localization or whether strain localization induces damage. Nevertheless one can conclude that damage nucleation is strongly related to fracture without void growth step. Furthermore, one can conclude that the macroscopic strain inducing cleavage at 320 °C is about 15% and is higher than the one at 20 °C: this leads to higher fracture strain in tension at 320 °C.

In compression tests, the origin of the macroscopic fracture is questionable. It is well known that the friction between specimen and machine leads to the shearing of the specimen. But a compressive test was performed on a 321 stainless steel under the same conditions (same geometry and lubricant) as those used during the duplex stainless steel tests and no localization was found even for a height reduction of 50%. This confirms that the localization observed in the compressed specimen made of duplex stainless steel, is mainly associated with the mechanical behavior of the material, specially to dynamic aging, even though it is probably enhanced by the contact conditions.

Flow stress levels measured in tensile and in compression tests can be linked to damage and to mechanical behavior. At room temperature, the damage modifies the macroscopic flow stress under tensile stress. As a consequence the flow stress measured in tension is lower than the one measured in compression. At 320 °C, dynamic strain aging leads to fracture as soon as damage occurs. The flow stress level in tension and in compression are thus the same.

Up to now, introducing a negative strain rate sensitivity in a constitutive mechanical behavior law is still a challenge [30]. Coupling it with damage for the prediction of crack propagation resistance is even more difficult. To propose a damage model, the localization stage should be identified: it can occur before any promotion by damage nucleation, or during the void growth stage, or still in the post-coalescence process where localization also occurs at a microscopic scale. Local strain rate and temperature are essential parameters to bring an answer to this question. In this material and for the temperature and strain rate range used in this study, the damage nucleation can be considered as the major stage of the damage process since no large crack opening is observed. Moreover no bulk damage is observed at 320 °C unlike the observation at room temperature. A critical strain, the strain for damage nucleation, can thus be proposed as a local fracture criterion. In the case of localization induced by damage, a phenomenological way to represent it in the framework of Gurson's type model, could be to consider only the damage nucleation and omit void growth and void coalescence: damage nucleation leading directly to strain and damage localization and fracture.

5. Conclusions

At room temperature, typical steps of damage were observed in tensile loading. Columnar specimens exhibited a larger scatter of the fracture strain than equiaxed ones because of the coarser solidification structure. Cleavage cracks parallel to the material flow direction were observed on longitudinal sections of the compressed specimens. This confirms that damage kinetic is driven by the plastic strain in this material.

At 320 °C, the damage of the duplex stainless steel in tension consisted of cleavage, shearing and ductile fracture in ferrite. Cleavage in ferrite at 320 °C occurred at higher strain than at 20 °C. No difference could be noticed, in tension or in compression, for equiaxed and columnar grain specimens. The major feature of aged duplex stainless steel tested at 320 °C under a strain rate of 3×10^{-4} s^{-1} was dynamic strain aging. Because of this phenomenon, the deformation is unstable and localized. As a consequence, there was no bulk damage in tension below the fracture surface. It seems thus not really appropriate to use local approach models based on the description of void growth. Since damage nucleation is controlled by the macroscopic plastic strain and damage nucleation is closely associated with the final fracture, a critical strain can be proposed as a local fracture criterion.

Acknowledgements

Electricité De France is gratefully acknowledged for its financial support and material supply.

References

[1] R.M. Fischer, E.J. Dulis, K.G. Carroll, J. Metals (1953) 660.
[2] P.J. Grobner, Metall. Trans. 4 (1973) 251.
[3] P. Auger, F. Danoix, A. Menand, S. Bonnet, J. Bourgoin, M. Guttman, Mater. Sci. Tech. 6 (1990) 301.
[4] S. Bonnet, J. Bourgoin, J. Champredonde, D. Guttmann, M. Guttmann, Mater. Sci. Tech. 6 (1990) 221.
[5] H.M. Chung, T.R. Leax, Mater. Sci. Tech. 6 (1990) 249.
[6] P. Auger, F. Danoix, J.P. Massoud, M. Guttmann, in: P. Berge, G. Zacharie (Eds.), Endommagement des matériaux dans les centrales nucléaires à eau pressurisée, Eyrolles, p. 23.

[7] S. Jayet-Gendrot, P. Gilles, C. Migné, Nucl. Eng. Des. 197 (2000) 141.
[8] P. Haušild, C. Berdin, P. Bompard, N. Verdière, Int. J. Pres. Ves. Piping 78 (2001) 607.
[9] J.P. Massoud, M. Bethmont, J. Champredonde, in: Proceedings of International Conference on Duplex Stainless Steels, Beaune, France, 1991.
[10] S. Jayet-Gendrot, P. Ould, T. Meylogan, Nucl. Eng. Des. 184 (1998) 3.
[11] Standard test method for measurement of fracture toughness, ASTM E 1820-99.
[12] A. Gurson, J. Eng. Mater. Tech. 99 (1977) 2.
[13] V. Tvergaard, J. Mech. Phys. Sol. 30 (1982) 399.
[14] V. Tvergaard, A. Needleman, Acta Metall. 32 (1984) 157.
[15] P. Joly, A. Pineau, Y. Meyzaud, in: Proceedings of International Seminar on Micromechanics of Materials, Moret s/Loing, France, 6–7 July 1993, Eyrolles, p. 210.
[16] J. Besson, L. Devillers-Guerville, A. Pineau, Eng. Fract. Mech. 67 (2000) 169.
[17] C. Duval, D. Baptiste, C. Prioul, D. François, in: Proceedings of 8th European Conference on Fracture, Torino, Italy, 1–5 October 1990, EMAS, p. 388.
[18] P. Joly, PhD thesis, Ecole Nationale Supérieure des Mines de Paris, France, 1992.
[19] V. Calonne, A.F. Gourgues, A. Pineau, Fat. Fract. Eng. Mater. Struct. in press.
[20] G.V. Kurdjumov, G. Sachs, Z. Phys. 64 (1930) 325.
[21] S. Bugat, J. Besson, A.F. Gourgues, F. N'Guyen, A. Pineau, Mater. Sci. Eng. A 317 (2001) 32.
[22] J.M. Alegre Calderon, PhD thesis, Universidad de Cantabria, Spain, 2000.
[23] P.F. Thomason, Ductile Fracture of Metals, Pergamon, 1990.
[24] V. Calonne, PhD thesis, Ecole Nationale Supérieure des Mines de Paris, France, 2001.
[25] S. Degallaix-Moreuil, Thesisès Sciences Physiques, Université des Sciences et Techniques de Lille, France 1986.
[26] P. Hahner, Mater. Sci. Eng. A 207 (1996) 208.
[27] P. Delobelle, Int. J. Plast. 9 (1993) 65.
[28] D. Wagner, J.C. Moreno, C. Prioul, J.M. Frund, B. Houssin, J. Nucl. Mater. 300 (2002) 178.
[29] L.P. Kubin, Y. Estrin, Acta Metall. 33 (1995) 397.
[30] S. Kok, M.S. Bharathi, A.J. Beaudoin, C. Fressengeas, G. Ananthakrishna, L.P. Kubin, M. Lebyodkin, Acta Mater. 51 (2003) 3651.